

반응성 필러로써 Aluminum Fumarate를 이용한 Dicyanate Composites의 물성 강화: 열역학적 특성 연구

Siva Kaylasa Sundari Saravanamuthu^①, Shamim Rishwana Syed Mohammed^②, Ramani Ramasubbu*,
Arunjunai Raj Mahendran**, and Vijayakumar Chinnaswamy Thangavel***,†^③

Department of Chemistry, Kamaraj College of Engineering and Technology (Autonomous)

*Defence Bio-Engineering and Electromedical Laboratory, ADE Campus,

**Kompetenzzentrum Holz GmbH (W3C)

***Department of Polymer Technology, Kamaraj College of Engineering and Technology (Autonomous)

(2021년 8월 27일 접수, 2022년 4월 30일 수정, 2022년 5월 20일 채택)

Particulate Reinforcements in Dicyanate Composites with Nanoporous Aluminum Fumarate as Reactive Filler: Thermal Properties

Siva Kaylasa Sundari Saravanamuthu^①, Shamim Rishwana Syed Mohammed^②, Ramani Ramasubbu*,
Arunjunai Raj Mahendran**, and Vijayakumar Chinnaswamy Thangavel***,†^③

Department of Chemistry, Kamaraj College of Engineering and Technology (Autonomous),

S.P.G.C. Nagar, K. Vellakulam-625701, Tamil Nadu, India

*Defence Bio-Engineering and Electromedical Laboratory, ADE Campus, C.V. Raman Nagar, Bengaluru-560093, Karnataka, India

**Kompetenzzentrum Holz GmbH (W3C), Klagenfurter Straße 87-89, A-9300 St. Veit an der Glan, Austria

***Department of Polymer Technology, Kamaraj College of Engineering and Technology (Autonomous),

S.P.G.C. Nagar, K. Vellakulam-625701, Tamil Nadu, India

(Received August 27, 2021; Revised April 30, 2022; Accepted May 20, 2022)

Abstract: In this work, the synthesized nanoporous aluminum fumarate (Al₂FA₂) metal organic framework (MOF) has been used as reactive filler for the bisphenol-A dicyanate (BADCy) resin system. The use of Al₂FA₂ is interesting due to the involvement of double bonds (fumarate) in triazine during polymerization. The thermal properties of the polymers formed with and without reactive filler were evaluated under different curing temperatures, prepolymerizations and post-polymerizations conditions. All the samples were characterized by Fourier transform infrared spectroscopy (FTIR), thermogravimetric analysis (TGA), differential scanning calorimetry (DSC) and X-ray diffraction analysis (XRD) and Evolved gas analysis. On the contrary, the cure chemistry was determined by non-isothermal model free kinetic methods. This study provides a new path to utilize the MOFs as reactive nanoparticle fillers to obtain multifunctional materials.

Keywords: particle reinforcement, high-temperature properties, thermal analysis, hybrid nanocomposite.

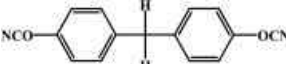
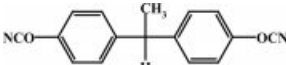
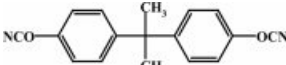
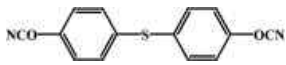
Introduction

High-temperature polymers are specialty materials that retain their properties after prolonged high-temperature exposure under static and/or dynamic conditions.¹ The demands in the electronics and aerospace industries necessitated the development of several high-temperature polymer systems.² Intensive research on epoxy resins, phenolic resins, and bismaleimide

resins were investigated. Each of the above resins has its unique properties with some drawbacks for their application as high-temperature polymers.³ Cyanate ester resins (CE) emerged as a novel material for use in high-temperature applications. The term cyanate ester resin which is also called cyanate resins, cyanic esters or triazine resins refers to the family of monomers and oligomers with reactive cyanate end functional groups (-O-C≡N). On thermal treatment or the addition of the catalyst, cyanate functional groups will homopolymerize into a polycyanurate.^{4,5} The polycyanurate materials have high strength and toughness, high glass transition temperature, low water absorption, low dielectric constant and good adhesion to a vari-

†To whom correspondence should be addressed.
cviijay22@yahoo.com, ORCID[®]0000-0001-6959-7165
©2022 The Polymer Society of Korea. All rights reserved.

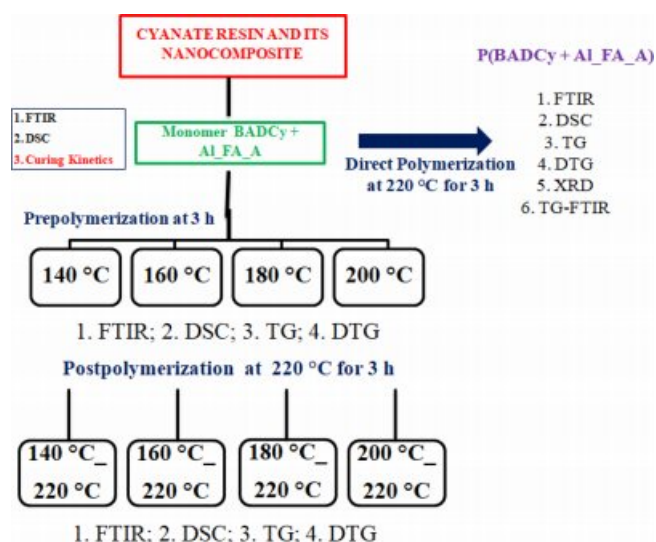
Table 1. Commercially Available Cyanate Resins

S.No.	Compound	Trade name
1	 Bisphenol F Dicyanate	Primaset METHYLCy (Lonza)
2	 Bisphenol E Dicyanate	Primaset LECy (Lonza) AroCy L-10 (Huntsman)
3	 Bisphenol A Dicyanate	BADCy AroCy B-10 (Huntsman)
4	 Bis(4-cyanatophenyl)sulfide	AroCy T-10 (Huntsman)

ety of substrates⁶ and they combine the advantages of epoxies, fire resistance of phenolics and high-temperature performance of polyimides.⁷ Hence they are widely used in the aerospace⁶ and electronic industries which were once dominated by epoxy resin systems. Researchers conducted various studies on the synthesis of CE resins with different solvents and catalysts.⁸⁻¹¹ The various types of cyanate systems with their trade names are given in Table 1. Among the cyanate resins (Table 1), Bisphenol A dicyanate (2,2-Bis(4-cyanatophenyl)propane, BADCy) was the first and the least expensive cyanate monomer to be commercialized. The BADCy resins are organic compounds that are generally manufactured from cyanogen halides and bisphenol-A. Various transition metal salts or chelates are added either as a catalyst or filler to cyanate systems for polymerization.¹²

Numerous literature contains information regarding the composite materials of various cyanate esters blended with epoxy,¹³⁻¹⁶ bismaleimide resins,^{17,18} benzoxazines,²⁰ rubbers,²¹ and fillers.²² The reinforcement of inorganic materials which includes aluminum phosphate, aluminum nitride,^{23,24} aluminum borate whiskers, alumina/Silica nanoparticles,^{25,26} etc. in CE resin systems were also studied.

This research work plans to incorporate the nanoporous metal organic frameworks (MOFs) into the BADCy resin. MOFs are a new class of crystalline porous materials made from the inorganic part (metal node) and organic part (organic linker) preferably diacids and functionalized diacids.²⁷ MOFs are the hopeful candidates for a variety of applications especially in the field of gas storage and catalysis^{28,29} because of their extraordinary pore size and high surface area. Aluminum

**Scheme 1.** Overall scheme for this work of neat resin, oligomers and the hybrid nanocomposite.

is one of the most promising materials in recent years and the studies regarding the aluminum-based catalyst are copious.³⁰⁻³² Therefore aluminum is selected as a metal node and fumaric acid is used as an organic linker. The detailed studies of the self-assembled synthesis of aluminum fumarate (Al_FA_A) were done in our previous work.³³ The present investigation generally relates to the high-performance hybrid nanocomposite which was developed using BADCy and Al_FA_A as reactive nanoparticle filler. The overall scheme for the paper-work is summarized in Scheme 1. Similar work was followed for the BADCy system.

Experimental

Materials. The compounds Bisphenol A dicyanate and the nanoporous aluminum fumarate MOF were synthesized. The materials were used after purification. All the other chemicals and solvents were used as such received.

Synthesis of Dicyanate Ester (BADCy): The synthetic procedure is given in Supplement S. The scheme for synthesis and its microscopic image are given in Figure 1. The synthesis of aluminum fumarate was already reported in our previous work.³³

Preparation of Hybrid Nanocomposites: The dicyanate ester/MOF hybrid nanocomposite was prepared by blending BADCy with 1% nanoporous Al_FA_A without the aid of any solvents. The prepolymerizations of the cyanate ester resin (BADCy) and the hybrid composite (BADCy+Al_FA_A)

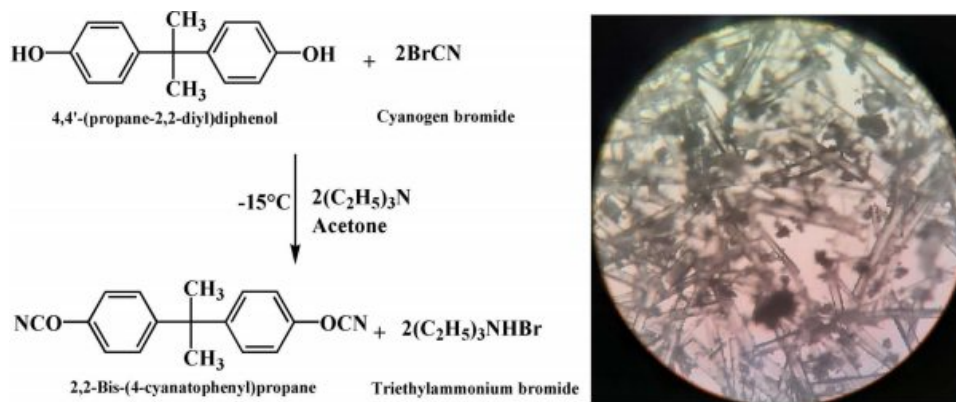


Figure 1. Synthesis and microscopic (40 \times) image of BADCy.

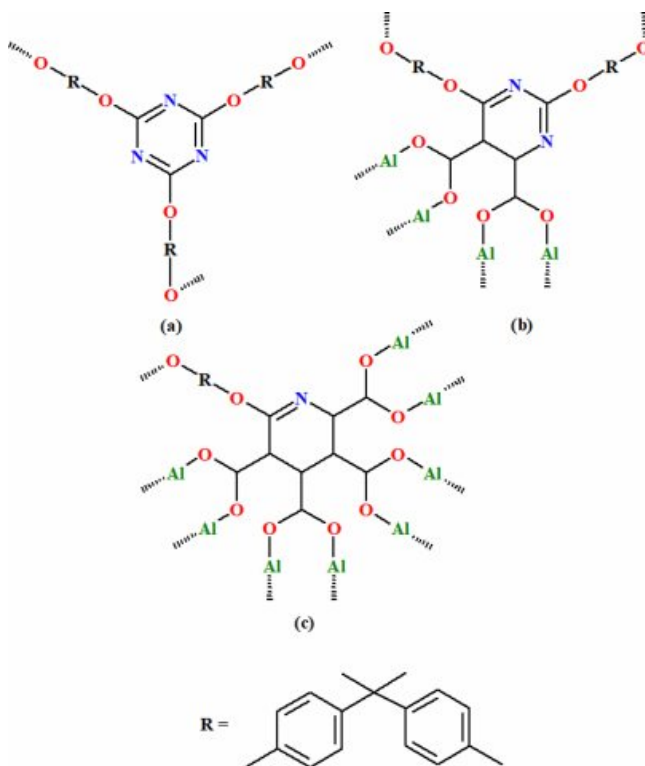


Figure 2. Mechanistic approaches for the polymerization of (a) BADCy; (b, c) hybrid nanocomposite.

were done at various temperatures (140 $^{\circ}\text{C}$, 160 $^{\circ}\text{C}$, 180 $^{\circ}\text{C}$, and 200 $^{\circ}\text{C}$) for a constant period of 3 h. All the prepolymerized samples are postpolymerized at a constant temperature of 220 $^{\circ}\text{C}$ for 3 h. The polymerization mechanisms of BADCy without reactive nanofiller - Figure 2(a) and with reactive nanofiller - Figure 2(b and c) are given in Figure 2.

Methods. The Fourier transform infrared spectrum (FTIR) of the material was recorded on a Fourier transform infrared-8400S spectrophotometer, Shimadzu, Japan using the potas-

sium bromide disc technique. The differential scanning calorimetric (DSC) curves were recorded using TA Instruments DSC Q20 using a non-hermetic aluminum pan. The samples were heated from ambient to 350 $^{\circ}\text{C}$ at 10 $^{\circ}\text{C}/\text{min}$ in a nitrogen atmosphere (50 mL/min). For curing kinetic studies, the samples were heated at different heating rates ($\beta=5, 10, 15$ and 20 $^{\circ}\text{C}/\text{min}$) from ambient to 350 $^{\circ}\text{C}$ in a nitrogen atmosphere. The thermal degradation behavior of the material was examined using TGA Model Q50 supplied by TA Instruments, Waters India Pvt., Ltd., Bengaluru - 560086, India. The measurements were carried out using approximately 3-4 mg of the sample in a high purity nitrogen atmosphere and the flow of nitrogen to the balance area was 40 mL/min and the sample was swept with a nitrogen flow of 60 mL/min. Similar flow conditions were maintained for recording the TG curves in the air atmosphere. The obtained TG and DTG curves were analyzed using the universal analysis 2000 software provided by TA instruments. X-ray diffractogram (XRD) was recorded in the Philips PANalytical XPERT-PRO X-Ray diffractometer operating at a voltage of 40 kV, current of 30 mA and Cu target having a wavelength as 1.5418 \AA . The polymerized sample was scanned from $2\theta=5$ to 90 $^{\circ}$. The TG-FTIR study of polymerized samples of BADCy and its hybrid nanocomposite was carried out in a TA Instruments TGA Q5000 V3.10 Build 258 at a heating rate of 10 $^{\circ}\text{C}/\text{min}$ from ambient to 800 $^{\circ}\text{C}$. Nearly, 3-4 mg samples were used for the analysis in the nitrogen atmosphere (balance flow: 10 mL/min and sample flow: 25 mL/min) and the FTIR spectra of the volatiles formed during the thermal degradation were recorded for every 30 s. Thermal analysis kinetics (TAK) seeks to analyze kinetic parameters, the lifespan of materials and the best-operating conditions for the materials. Supplement S summarizes the most commonly used reliable model free kinetic methods for curing kinetics.

Results and Discussions

FTIR Studies. The FTIR spectrum of monomers - BADCy and its hybrid nanocomposite BADCy+Al_FA_A, prepolymers of both the compounds at various temperatures, post-polymerizations and directly polymerized compounds -P(BADCy) and P(BADCy+Al_FA_A) are represented in Figure 3. The frequency and its corresponding bands of the bisphenol-A-based dicyanate ester resin system are given in Table 2.

The compound BADCy shows the phenolic -OH stretching at 3139 cm^{-1} , C-H stretching in $-\text{CH}_3$ at 2979 cm^{-1} , cyanate ($-\text{C}\equiv\text{N}$) stretching at 2272 cm^{-1} , carbamate stretching at 1730 cm^{-1} and C-O-C stretching at 1197 cm^{-1} . Along with inter and intramolecular H-bond (3471 and 3128 cm^{-1}), the blend of BADCy and Al_FA_A hybrid nanocomposite shows similar bands of BADCy resin system. Once the polymerization was initiated, the increase in the intensity of the bands at 1510 cm^{-1} ($-\text{C}=\text{N}-\text{C}$) and 1400 cm^{-1} ($-\text{O}-\text{C}=\text{N}$) responsible for the triazine group, $1240\text{--}1100\text{ cm}^{-1}$ of the C-O-C group and the subsequent decrease of $-\text{C}\equiv\text{N}$ stretching (2240 to 2260 cm^{-1}) band confirms the polymerization. The pre-polymerizations of BADCy at various temperatures confirm that polymerization happens via the trimerization of the cyanate groups. The $\text{C}=\text{C}$ stretch at 1600 cm^{-1} (Blue in Figure 3); the $=\text{C}-\text{H}$ out of a plane at 800 cm^{-1} and bending vibrations at 1000 cm^{-1} in fumarate units (Pink in Figure 3) decreases during the pre-polymerization and it completely disappears in the post polymerizations. This indicates that the Al_FA_A enters into the trimerization process of BADCy.³⁴ The mechanism of trimerization of cyanate and the involvement of double bonds of fumarate in trimerization is given in Figure 2. Huang *et al.*¹³ confirmed the interaction of epoxy with the cyanate ester through the decomposition of triazine followed by the conversion of oxazolidone into oxazoline.

Table 2. The Frequency and Corresponding Bands of Cyanate Ester Systems

S.No.	Frequency (cm^{-1})	Bands
1	3100	Phenolic -OH stretching
2	2970	C-H stretching in CH_3
3	2240 to 2260	$\text{C}\equiv\text{N}$ stretching
4	1510	$\text{C}=\text{N}-\text{C}$ stretching of triazine ring ³⁴
5	1400	$\text{O}-\text{C}=\text{N}$ stretching of triazine ring ^{34,35}
6	1100 to 1200	C-O-C stretching
7	820	C-H out of plane deformation

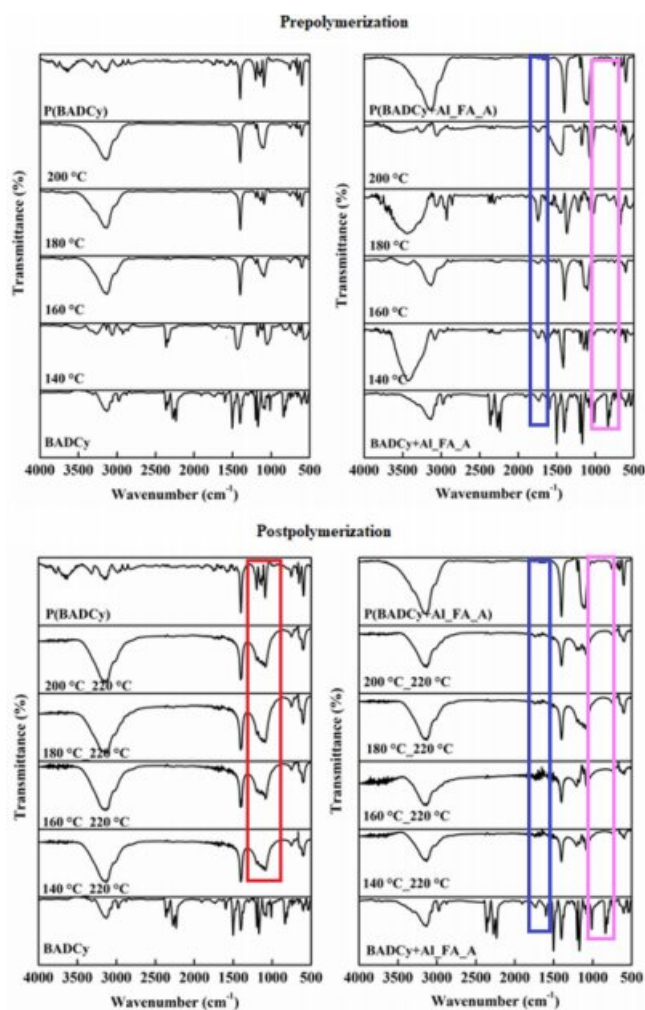


Figure 3. Comparison of Monomers, Prepolymerizations at various temperatures, Postpolymerizations and Direct polymerization of BADCy and BADCy+Al_FA_A.

The postpolymerization of BADCy follows a similar pattern of polymerization (red in Figure 3) but the hybrid nanocomposite polymerization occurs differently for every post-polymerization. This indicates that the nanoporous MOF in the BADCy resin matrix has a profound effect on the polymerization mechanism. The direct polymerized BADCy (P(BADCy)) and its hybrid nanocomposite show new peaks of triazine and C-H out of plane deformation at 820 cm^{-1} .

DSC Studies. The DSC thermograms for the monomer BADCy and the BADCy+Al_FA_A blend are given in Figure 4. The details regarding the melting and curing of both the monomers are given in Table 3. From the DSC thermogram, BADCy shows a melting at $82\text{ }^\circ\text{C}$ and the addition of MOF nanoparticles decreases the melting temperature by $2\text{ }^\circ\text{C}$. The heat of fusion (ΔH_f) for BADCy (31 J/g) was reduced to half

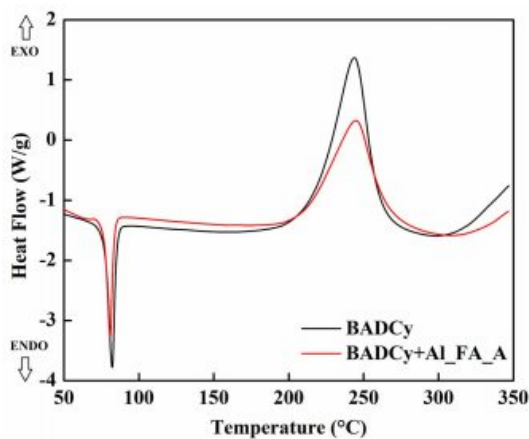


Figure 4. The DSC thermogram of the BADCy and BADCy+Al_FA_A.

for the blend (16 J/g).

The BADCy shows the onset curing temperature (T_s) at 196 °C, the temperature at which the curing rate is maximum (T_{max}) at 252 °C and the endset temperature (T_E) at 334 °C. The addition of nanoporous material decreases the onset curing temperature to 192 °C, the temperature at which the curing rate is maximum to 243 °C and the endset temperature to 329 °C. The enthalpy of curing (ΔH_c) for BADCy is 211 J/g whereas incorporation of Al_FA_A in BADCy drastically decreases the value to 86 J/g which amounts to a decrease of 59%. The reduction in the ΔH_f and ΔH_c values for the blend indicates the interaction existing between the organic and inorganic components in the blend. The T_E-T_s values of both the pure resin and the blend show an almost similar rate of curing. From the DSC curves of BADCy and the blend (BADCy+Al_FA_A), it is understood that the physical blending of the nanoporous aluminum fumarate MOF to resin has a profound effect on the matrix.

Table 3. Parameters Derived from the DSC Curves of Monomer – BADCy and Its Blend with Aluminum Fumarate (BADCy+Al_FA_A)

Sample code	T_m (°C)	ΔH_f (J/g)	T_s (°C)	T_{max} (°C)	T_E (°C)	T_E-T_s (°C)	ΔH_c (J/g)
BADCy	82	31	196	252	334	138	211
BADCy+Al_FA_A	80	16	192	243	329	137	86

DSC Curves of Prepolymerized BADCy and BADCy+Al_FA_A: The curing behaviors of the prepolymerized oligomers of BADCy and the BADCy+Al_FA_A are studied by DSC and it is presented in Figure 5. The values of curing parameters of different materials investigated are given in Table 4. Compared to the monomer, the prepolymerized sample at 140 °C (3 h) of BADCy and its blend shows a notable decrease in the curing onset temperature by 27 and 42 °C; maximum curing temperature by 13 and 8 °C; endset curing temperature by 37 and 30 °C respectively. All the other prepolymerized samples at 160, 180, and 200 °C (3 h) exhibit a gradual increase in the DSC parameters like T_s , T_{max} and T_E . The curing window decreases in both the monomers and the hybrid nanocomposite when the pre-polymerization temperature increases.

The enthalpy of curing increases for pre-polymerization at 140 °C for 3 h by 118 and 396 J/g for resin and hybrid material respectively and a drastic decrease was observed in all the other prepolymerized samples.

Curing Kinetics – Model Free Methods. Several authors reported the curing and degradation kinetics of various cyanate resins.³⁶⁻³⁹ The incorporation of the metal organic framework as reactive nanoparticle filler and its characterization is presented for the first time in this work. Siva Kaylasa Sundari *et*

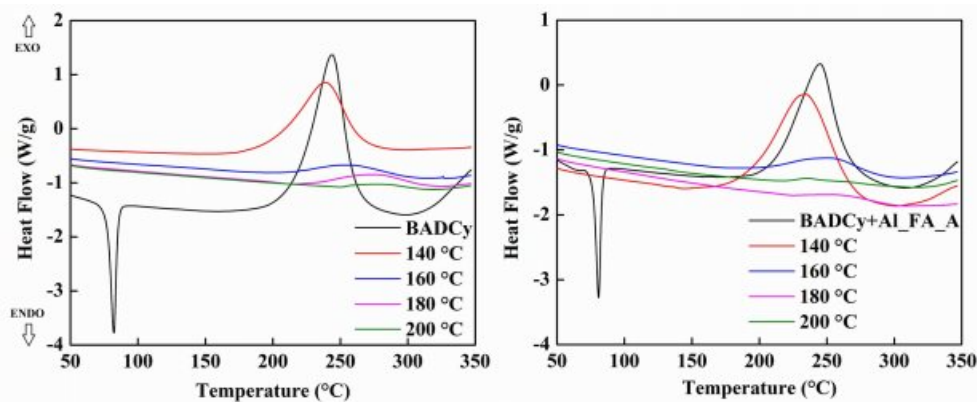


Figure 5. DSC thermograms of the monomer (BADCy) and (BADCy+Al_FA_A) with their prepolymers at various temperatures.

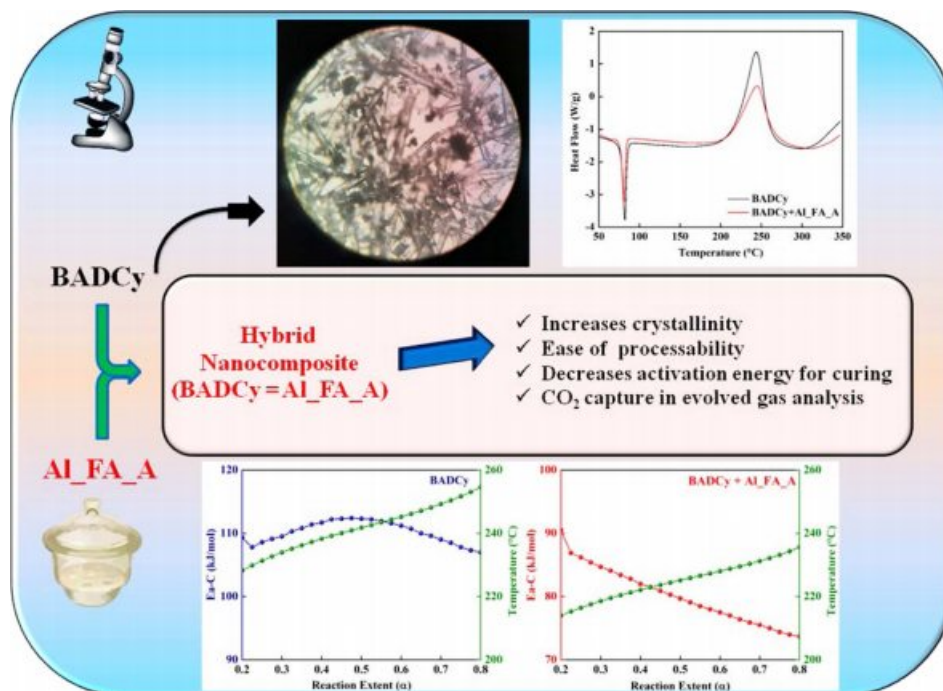
Table 4. Parameters Derived from the DSC Curves of Monomers and Prepolymers of BADCy and Its Hybrid Nanocomposite

Sample code	T_m (°C)	ΔH_f (J/g)	T_s (°C)	T_{max} (°C)	T_E (°C)	T_E-T_s (°C)	ΔH_c (J/g)
BADCy	82	31	196	252	334	138	211
BADCy_140 °C	-	-	169	239	297	128	329
BADCy_160 °C	-	-	207	260	310	103	57
BADCy_180 °C	-	-	214	274	316	102	55
BADCy_200 °C	-	-	247	283	323	76	16
BADCy+Al-FA_A	80	16	192	243	329	137	86
BADCy+Al-FA_A_140 °C	-	-	150	235	299	149	482
BADCy+Al-FA_A_160 °C	-	-	191	255	301	110	69
BADCy+Al-FA_A_180 °C	-	-	216	261	307	79	19
BADCy+Al-FA_A_200 °C	-	-	218	238	308	91	16

al. already had an experience in thermal degradation kinetics for various polymers and biomolecular brushes which finds application in the field of tissue engineering.⁴⁰ The apparent activation energy for curing of BADCy is in the region of 110 to 120 kJ/mol whereas the Ea-C values of the blend lie from

75 to 90 kJ/mol. This decrease noted in Ea-C values for BADCy+Al_FA_A confirms the difference in the curing behavior of the materials studied. The probable interaction of the fumarate π bonds with the π bonds presented in the -O-C \equiv N of the cyanate ester may be the reason for this observation. The Scheme for the XRD, curing kinetics and the evolved gas analysis are presented in Scheme 2. Kimura *et al.*²⁰ studied the curing kinetics of bisphenol-A based benzoxazine with the bisphenol-A based cyanate ester. The authors found that the phenolic hydroxyl group produced by ring opening reaction of benzoxazine co-reacted with cyanate ester group to form the iminocarbonate, which further induce curing reaction of cyanate ester to form polycyanurate.

Comparison of TG and DTG in the air (A), (B) and Nitrogen (C), (D). The thermal analyses of the polymerized samples are studied under two different conditions (air and nitrogen) and it is presented in Figure 6. In the air atmosphere, the P(BADCy) and P(BADCy+Al_FA_A) show two distinguishable degradations and it shows 2 and 6% char residue respectively. But in a nitrogen atmosphere, both the polymerized samples exhibit single degradation. This proves that the second degradation in the air atmosphere is the oxidative degradation of the polymerized materials.⁴¹ The presence of MOF as reactive filler decreases the thermal stability of the BADCy system in both air and nitrogen atmosphere. Degradation


Scheme 2. The scheme represents the highlights of hybrid nanocomposite.

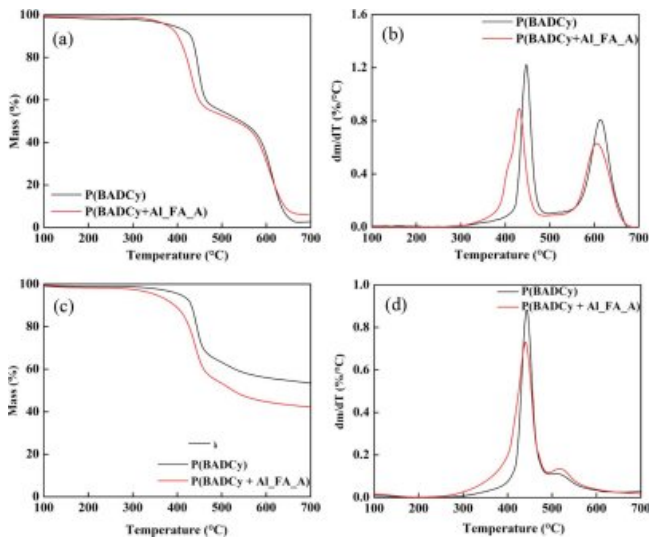


Figure 6. Comparison of TG and DTG curves of polymerized BADCy and hybrid nanocomposite in the air (a, b); nitrogen (c, d).

parameters of P(BADCy) and hybrid nanocomposite P(BADCy+Al_FA_A) in Air and Nitrogen are given in Table 5. The incorporation of MOF in BADCy leads to a slight decrease in thermal stability due to the probable degradation of the fumarlyl part of the MOF. The TG for prepolymerized and post-

polymerized samples of BADCy and its hybrid nanocomposite are discussed in detail in the supplement.

TG-FTIR. The evolved gas analysis for the polymerized BADCy and its hybrid nanocomposite are presented in Figure 7. From the figures, it is evident that the profile of the absorbance band noted at 2400 cm^{-1} may be safely assigned to the evolution of CO_2 from the degrading materials. The evolution of CO_2 starts at around $350\text{ }^\circ\text{C}$ and becomes sufficiently very low at $800\text{ }^\circ\text{C}$ and the maximum evolution of CO_2 was observed at the temperature region of $370\text{--}410\text{ }^\circ\text{C}$. It is interesting to note that the decrease in the intensity of the CO_2 evolution confirms that MOF can capture the evolved CO_2 in the tunnels of the frameworks. This decrease in intensity was seen in the scale and the 2-D TG-FTIR (Supplement Figure S13) of P(BADCy) and P(BADCy+Al_FA_A). The main degradation occurs at 44 min ($370\text{ }^\circ\text{C}$) in both P(BADCy) and P(BADCy+Al_FA_A).

The FTIR spectra of the evolved gases from both these materials are presented in Figure S14. The evolved gas analysis along with characterizations and the thermal degradation kinetics for aluminum fumarate was reported in our previous work.³³ The polymerized compounds released benzene, ethylbenzene, phenol, cumene and substituted alkenyl benzenes.

Table 5. Degradation Parameters of P(BADCy) and Hybrid Nanocomposite P(BADCy + Al_FA_A) in Air and Nitrogen

Sample code	First degradation stage				Second degradation stage				Residue (%)
	T_S (°C)	T_{max} (°C)	T_E (°C)	Mass loss (%)	T_S (°C)	T_{max} (°C)	T_E (°C)	Mass loss (%)	
P(BADCy) - Air	358	439	494	41	543	616	678	57	2
P(BADCy) - Nitrogen	376	443	623	45	-	-	-	-	53
P(BADCy + Al_FA_A) - Air	302	431	489	45	526	608	690	47	6
P(BADCy + Al_FA_A) - Nitrogen	327	439	658	55	-	-	-	-	42

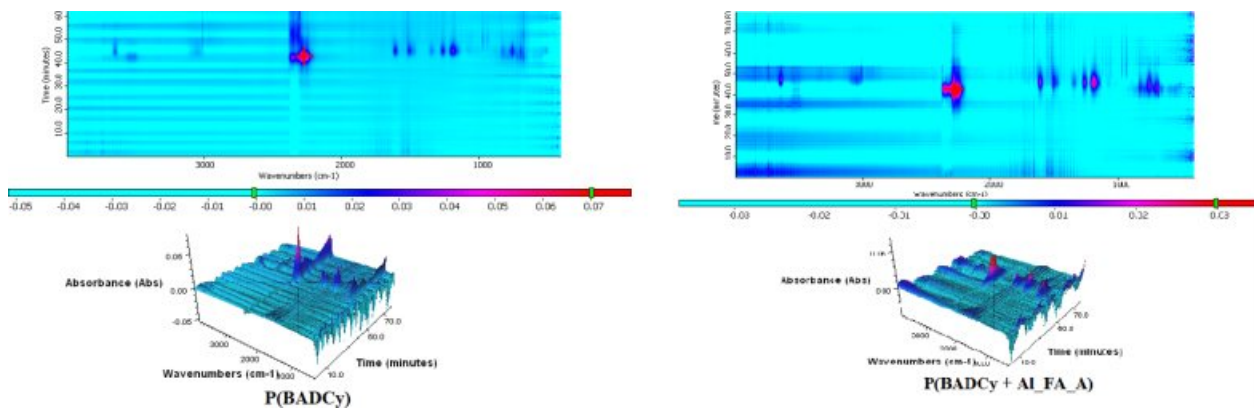
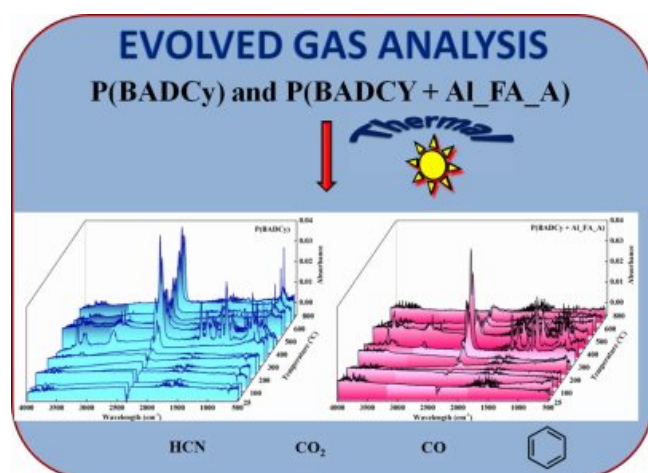


Figure 7. Contour plot and 3-D representation for P(BADCy+Al_FA_A).



Scheme 3. 2D TG-FTIR and products evolved during degradation.

The degradation of polymerized samples also released N_2 , CO_2 , CO and HCN . The scheme included 2D TG-FTIR and the products evolved during the degradation of BADCy and its hybrid particulate nanocomposite are given in Scheme 3.

Conclusions

The BADCy was prepared in the presence of triethylamine from diphenol (Bisphenol A) and cyanogen bromide. The Al_FA_A MOFs which was used as reactive nanoparticle filler was synthesized in an eco-friendly manner. The prepolymerized oligomers of the BADCy and the hybrid nanocomposite (BADCy+Al_FA_A) were obtained at various temperatures. The postpolymerizations were also done for every prepolymerized oligomer. These oligomers and the postpolymerized samples were characterized by FTIR and their thermal properties were evaluated using DSC and TG. The effect of nanoporous MOF addition on the curing behavior of the dicyanate resin system has been studied by DSC. The apparent activation energy for curing (E_a -C) of BADCy is in the region of 110 to 120 kJ/mol whereas the E_a -C values of the blend lie in the region of 75 to 90 kJ/mol. This decrease noted in E_a -C values for BADCy+Al_FA_A confirms the difference in the curing behavior of the materials and the probable interaction of the fumarate π bonds with the π bonds presented in the $-O-C\equiv N$ of the cyanate ester may be the reason for this observation. The shelf lifetime for BADCy polymerized to a level of 20% ($\alpha=0.2$) is 10000 h at 66 °C. But the same shelf lifetime of 10000 h is possible in the case of the MOF blended BADCy at the temperature of 39 °C. This difference is a clear indication of the interaction that is existing between the organic and the

inorganic parts of the blend. The addition of nanoporous aluminum fumarate material to the BADCy matrix decreases the initial degradation temperature by 50 °C irrespective of the atmosphere used for degradation (Nitrogen and Air). From evolved gas analysis (TG-FTIR), a reduction in the CO_2 evolution from the cured blend confirms the entrapment of evolved volatiles in the tunnels of aluminum fumarate MOF. This detailed study on MOF-based hybrid nanocomposite is opening new avenues of detailed scientific investigations regarding the use of nanoporous materials as reactive nanofillers for advanced high-temperature thermoset resin systems.

Acknowledgements: S. Siva Kaylasa Sundari – Methodology, Writing Original Draft; S. Shamim Rishwana – Supervision, Writing – review & editing, R. Ramani - Funding acquisition, Arunjunai Raj Mahendran - TG-FTIR investigation and Dr. C.T. Vijayakumar – Conceptualization, Writing – review & editing. All authors have approved the final version of the manuscript.

The authors express their sincere thanks to the Management and Principal of Kamaraj College of Engineering and Technology (Autonomous), S.P.G. C. Nagar, K. Vellakulam-625701 Madurai, India for providing all of the facilities to do the work. One of the authors (SKS) thanks DEBEL-DRDO for the financial assistance in the form of a Research Fellowship under the CARS project. This work was supported by Defence Bio-Engineering and Electromedical Laboratory [grant number: DEBEL/12FYP/ALSP/CARS/003], ADE Campus, C.V. Raman Nagar, Bengaluru-560093, Karnataka, India through CARS project.

Conflict of Interest: The authors declare that they have no known competing financial interests or personal relationships that could have appeared to influence the work reported in this paper.

Supporting Information: A brief description regarding the curing kinetics to predict the apparent activation energy for curing, lifetime and pre-exponential factor are supplied as supporting information. The materials are available *via* the Internet at <http://journal.polymer-korea.or.kr>.

References

1. Hammerton, I. Chemistry and Technology of Cyanate Ester; Springer: Dordrecht, 1994.

2. Fink, J. K. *Reactive Polymers Fundamentals and Applications*; William Andrew Publishing: Norwich, **2006**.
3. Laurence, W. M. *The Effect of Long Term Thermal Exposure on Plastics and Elastomers*; William Andrew Publishing: Norwich, **2014**.
4. Clerici, C.; Gu, X. H.; Sung, L.; Forster, A. M.; Ho, D. L.; Stutzman, P.; Nguyen, T.; Martin, J. W. Effect of Pigment Dispersion on Durability of a TiO₂ Pigmented Epoxy Coating During Outdoor Exposure. In *Service Life Prediction of Polymeric Materials*; Martin, J. W., Ryntz, R. A., Chin, J., Dickie, R. A., Eds.; Springer: New York, 2009; pp 475-492.
5. Guenther, A. J.; Lamison, K. R.; Vij, V.; Reams, J. T.; Yandek, G. R.; Mabry, J. M. New Insights into Structure-Property Relationships in Thermosetting Polymers from Studies of Cured Polycyanurate Networks. *Macromolecules* **2012**, *45*, 211-220.
6. Sheng, X.; Akinc, M.; Kessler, M. R. Creep Behavior of Bisphenol E Cyanate Ester/Alumina Nanocomposites. *Mater. Sci. Eng., A* **2010**, *527*, 5892-5899.
7. Reghunadhan Nair, C. P.; Mathew, D.; Ninan, K. N. Cyanate Ester Resins, Recent Developments. *Adv. Polym. Sci.* **2001**, 1-99.
8. Liu, J.; Fan, W.; Lu, G.; Zhou, D.; Wang, Z.; Yan, J. Semi-Interpenetrating Polymer Networks Based on Cyanate Ester and Highly Soluble Thermoplastic Polyimide. *Polymers* **2019**, *11*, 862.
9. Oh, S.; Malpani, Y. S.; Jung, Y. S.; Kim, J. M. Photochemical Phase Transition Behavior of Supramolecular Polymer with a Triazine Core. *Polym. Korea* **2016**, *40*, 651-654.
10. Harvey, B. G.; Davis, M.; Lamison, K.; Cambrea, L.; Ford, M.; Haines, S.; Cash, J. *Cyanate Ester Composite Resins Derived from Renewable Polyphenol Sources*; ADD557386; US Navy, NAVAIR, Naval Air Warfare Center, Weapons Division : China Lake, CA, 2011.
11. Wang, F.; Wang, J.; Zhu, Y.; Zhang, Z.; Jiao, Y. Synthesis and Characterization of a Novel Cyanate Ester Containing Dimethyl Benzene Linkage. *Int. J. Polym. Anal. Charact.* **2010**, *15*, 415-423.
12. George, W. *Handbook of Fillers (Materials Science)*. 1999.
13. Huang, L.; Wang, C.; Lu, Y. Thermal and Moisture Adsorption Properties of Cyanate Ester Modified Epoxy Resin and Fiber-Glass Composites. *J. Reinf. Plast. Compos.* **2008**, *27*, 725-738.
14. Pietrowicz, S.; Four, A.; Jones, S.; Canfer, S.; Baudouy, B. Thermal Conductivity and Kapitza Resistance of Cyanate Ester Epoxy Mix and Tri-Functional Epoxy Electrical Insulations at Superfluid Helium Temperature. *Cryogenics* **2012**, *52*, 100-104.
15. Suguna Lakshmi, M.; Reddy, B. S. R. Synthesis and Characterization of New Epoxy and Cyanate Ester Resins. *Eur. Polym. J.* **2002**, *38*, 795-801.
16. Večeřa, M.; Prokůpek, L.; Machotová, J.; Šňupárek, J.; Husáková, L.; Urbanová, I.; Akštein, Z. Epoxy-Cyanate Ester Compositions as Matrixes for Tagging of Explosives. *Adv. Polym. Technol.* **2014**, *33*, 21399.
17. Shi, P.; Wang, Y.; Guo, H.; Sun, H.; Zhao, Y. The Thermal and Mechanical Properties of Carbon Fiber/flake Graphite/cyanate Ester Composites. *New Carbon Mater.* **2019**, *34*, 110-114.
18. Guo, Y.; Chen, F.; Han, Y.; Li, Z.; Liu, X.; Zhou, H.; Zhao, T. High-Performance Fluorinated Bismaleimide-Triazine Resin with Excellent Dielectric Properties. *J. Polym. Res.* **2018**, *25*, 27.
19. Wen, Y.; Yan, J.; Liu, J.; Wang, Z. Interpenetrating Polymer Networks Based on Cyanate Ester and Fluorinated Ethynyl-Terminated Imide Oligomers. *Express Polym. Lett.* **2017**, *11*, 936-945.
20. Kimura, H.; Ohtsuka, K.; Matsumoto, A. Curing Reaction of Bisphenol-A Based Benzoxazine with Cyanate Ester Resin and the Properties of the Cured Thermosetting Resin. *Express Polym. Lett.* **2011**, *5*, 1113-1122.
21. Yang, Z.; Peng, H.; Wang, W.; Liu, T. Crystallization Behavior of Poly(ϵ -Caprolactone)/layered Double Hydroxide Nanocomposites. *J. Appl. Polym. Sci.* **2010**, *116*, 2658-2667.
22. Baştürk, E.; Şen, F.; Kahraman, M. V.; Madakbaş, S. Bisphenol A (BADCy)/bisphenol P (BPDCy) Cyanate Ester/Colemanite Composites: Synthesis and Characterization. *Polym. Bull.* **2015**, *72*, 1611-1623.
23. Mi, Y. N.; Liang, G.; Gu, A.; Zhao, F.; Yuan, L. Thermally Conductive Aluminum Nitride-Multiwalled Carbon Nanotube/cyanate Ester Composites with High Flame Retardancy and Low Dielectric Loss. *Ind. Eng. Chem. Res.* **2013**, *52*, 3342-3353.
24. Li, Y.; Xu, G.; Guo, Y.; Ma, T.; Zhong, X.; Zhang, Q.; Gu, J. Fabrication, Proposed Model and Simulation Predictions on Thermally Conductive Hybrid Cyanate Ester Composites with Boron Nitride Fillers. *Composites Part A* **2018**, *107*, 570-578.
25. Ganguli, S.; Dean, D.; Jordan, K.; Price, G.; Vaia, R. Chemorheology of Cyanate Ester - Organically Layered Silicate Nanocomposites. *Polymer* **2003**, *44*, 6901-6911.
26. Jin Seob, K.; Young Sil, L.; Kwan Han, Y.; Jong Hun, H. Mechanical Properties and Thermal Conductivity of Polycarbonate Composite Containing Aluminum-exfoliated Graphite Nanoplatelet Hybrid Powder. *Polym. Korea* **2021**, *45*, 275-280.
27. Furukawa, S.; Reboul, J.; Diring, S.; Sumida, K.; Kitagawa, S. Structuring of Metal-Organic Frameworks at the Mesoscopic/macroscopic Scale. *Chem. Soc. Rev.* **2014**, 5700-5734.
28. Yanbei, H.; Zhoumei, X.; Fukai, C.; Zhou, G.; Lei, S.; Yuan Hu, WH. A Review on Metal-organic Hybrids as Flame Retardants for Enhancing Fire Safety of Polymer Composites. *Composites Part B* **2021**, *221*, 109014.
29. Archana, K.; Pillai, N. G.; Rhee, K. Y.; Asif, A. Superparamagnetic ZIF-67 Metal Organic Framework Nanocomposite. *Composites Part B* **2018**, *158*, 384-389.
30. Siva Kaylasa Sundari, S.; Shamim Rishwana, S.; Ramani, R.; Vijayakumar, C. T. Improvement in Electrical and Mechanical Properties of Di/trifunctional Epoxies-based Hybrid Composites Having Metal Organic Frameworks (MOFs) as Nanoparticulate filler. *MRS Commun.* **2021**, *12*, 250-256.
31. Chopra, I. S.; Chaudhuri, S.; Veyan, J. F.; Chabal, Y. J. Turning Aluminium into a Noble-Metal-like Catalyst for Low-Temperature Activation of Molecular hydrogen. *Nat. Mater.* **2011**, *10*, 884-889.

32. Whiteoak, C. J.; Kielland, N.; Laserna, V.; Escudero-ada, E. C.; Martin, E. A Powerful Aluminum Catalyst for the Synthesis of Highly Functional Organic Carbonates. *J. Am. Chem. Soc.* **2013**, 135, 1228-1231.
33. Siva Kaylasa Sundari, S.; Shamim Rishwana, S.; Kotresh, T. M.; Ramani, R.; Indu Shekar, R.; Vijayakumar, C. T. Effect of Structural Variation on the Thermal Degradation of Aluminium Fumarate: Nanoporous Metal Organic Framework (MOF). *J. Therm. Anal. Calorim.* **2022**, 147, 5067-5085.
34. Hangtao, C.; Beijum, Liu.; Yunfang, L.; Peng, L. Reconstruction of the Microstructure of Cyanate Resin by Using Prepared Cyanate Ester Resin Nanoparticles and Analysis of the Curing Kinetics Using Avrami Equation of Phase Change. *Appl. Sci.* **2019**, 9, 2365.
35. Gouthaman, S.; Venkatesh, M.; Stanley Olivier, K.; Suguna Lakshmi.; Hamerton, I. Examining the Thermal Degradation Behavior of a Series of Cyanate Ester Homopolymers. *Polym. Int.* **2019**, 68, 1666-1672.
36. Shilpi, T.; Chhagan Lal, G.; Kavita Srivastava, D. S. Simulation of the Thermal Degradation and Curing Kinetics of Fly Ash Reinforced Diglycidyl Ether Bisphenol A Composite. *J. Indian Chem. Soc.* **2021**, 98, 100077.
37. Zhao, L.; Hu, X. Autocatalytic Curing Kinetics of Thermosetting Polymers: A New Model Based on Temperature-dependent Reaction Orders. *Polymer* **2010**, 51, 3814-3820.
38. Sheng, X.; Akinc, M.; Kessler, M. R. Cure Kinetics of Thermosetting Bisphenol E Cyanate Ester. *J. Therm. Anal. Calorim.* **2008**, 93, 77-85.
39. Reghunadhan Nair, C. P.; Francis, T. Blends of Bisphenol-A-Based Cyanate Ester and Bismaleimide: Cure and Thermal Characteristics. *J. Appl. Polym. Sci.* **1999**, 74, 3365-3375.
40. Siva Kaylasa Sundari, S.; Shamim Rishwana, S.; Poornimadevi, S.; Vijayakumar, C. T. Synthesis of Macromolecular Brush and its Thermal Degradation Studies. *Int. J. Polym. Anal. Charact.* **2022**, 27, 147-157.
41. Tang, L.; Zhang, J.; Tang, Y.; Zhou, Y.; Lin, Y.; Liu, Z.; Kong, J.; Liu, T.; Gu, J. Fluorine/Adamantane Modified Cyanate Resins with Wonderful Interfacial Bonding Strength with PBO Fibers. *Composites Part B* **2020**, 186, 107827.

Publisher's Note The Polymer Society of Korea remains neutral with regard to jurisdictional claims in published articles and institutional affiliations.